Published by IOP Publishing for Sissa Medialab

Received: *September 6, 2019*
Revised: *November 7, 2019*
Accepted: *December 9, 2019*
Published: *January 15, 2020*

2020 JINST 15 P01011

A setup for study of co-deposited films

S.A. Krat,[1] **A.S. Popkov, Y.M. Gasparyan, Y.A. Vasina, A.S. Prishvitsyn and A.A. Pisarev**

National Research Nuclear University "MEPhI",
Kashirskoe sh. 31, Moscow, 115409, Russia

E-mail: stepan.krat@gmail.com

Abstract: A setup for investigation of thermal desorption spectra of gases accumulated in thin films deposited by plasma sputtering of solid targets is described. Deposition and thermal desorption spectroscopy (TDS) are performed in two different vacuum chambers separated by a gate valve with the sample transferred between the chambers in-vacuo. The temperature of the substrate for deposited films can be varied in the range of 300–800 K; and the deposition rate is controlled by a quartz microbalance. Thermal desorption of co-deposited gases is analyzed by a quadrupole mass spectrometer. Sputtering rate and evaporation of the film during TDS are measured by quartz microbalances. Three experiments are described 1) trapping of deuterium by the growing chemically active Li film with subsequent decomposition and evaporation of the film, 2) temperature dependent deuterium trapping in the growing W film resulting in trapping with several binding energies, and 3) chemical interaction of D-Li layer with water vapor leading to isotopic H-D exchange and chemical transformation of the deposited film.

Keywords: Counting gases and liquids; Instrument optimisation

[1]Corresponding author.

https://doi.org/10.1088/1748-0221/15/01/P01011

Contents

2020 JINST 15 P01011

1 Introduction

Erosion and re-deposition of plasma facing materials in fusion devices are critically important processes for many reasons, such as radiological safety and the lifetime of plasma facing components. One of the safety issues is the so-called co-deposition process, which is simultaneous deposition and mixing of several species, leading to trapping of fuel (radioactive tritium) in future fusion devices in fresh films re-deposited on plasma facing surfaces following their sputtering by plasma ions [1, 2]. Tritium accumulation in fusion reactor is under safety regulations; and tritium in the co-deposited films is considered as one of the main contributors to T accumulation in the International Thermonuclear Experimental Reactor ITER [3]. Hydrogen isotopes trapping in the co-deposits is the main channel of fuel accumulation also in current fusion devices. For example, in JET, large quantities of hydrogen isotopes accumulated in co-deposited films (both in absolute terms and relative to the amount of the eroded wall material) were observed even in hard-to-reach shadowed areas of the installation [4–6].

Currently, there is no clear understanding which material will be used for plasma-facing components in commercial fusion devices. Several proposals and fusion reactor concepts exist, with such a wide variety of wall materials as tungsten [7], liquid metals, such as lithium and tin [8–12], steels [13, 14], beryllium [15]. Some of the materials (particularly Li) are very active chemically with respect to hydrogen [16–18] and atmospheric gases [19–21]. This makes the validity of experiments on post mortem analysis of hydrogen retention in Li-H co-deposits questionable, due to significant film transformations provoked by chemical reactions. Moreover, changes in hydrogen isotopes content is possible even in chemically inert materials after their long time exposure in air [22]. To enhance reliability of gas analyses in co-deposited films in-vacuo experiments must be performed with no contact of deposited films with air after co-deposition.

This paper describes set-up MD-2 for in-vacuo analysis of thermal desorption of hydrogen from metal films deposited in hydrogen environment. Magnetron sputtering in deuterium gas was used to deposit metal films containing deuterium in a wide range of deposition parameters [23]. Thermal desorption spectroscopy (TDS) gives information about hydrogen behavior in metals, such as total hydrogen content, desorption mechanisms, and binding energies [24]. Special efforts devoted to quantitative measurements of the amount of the metal deposited and hydrogen release rate in TDS are described. The TDS analysis was accompanied by a quartz microbalance measurement of film evaporation during TDS. For demonstration of the setup capabilities, experiments on hydrogen accumulation in various co-deposited films, and interaction of co-deposited films with gases are described.

2 Experimental setup

Figure 1 shows a schematic diagram of the setup. There are two main vacuum chambers: deposition chamber (1) and TDS chamber (2), separated by a vacuum gate valve (3). The sample (4) mounted on the feedthrough (5) moves between the two chambers. Film deposition is performed by using a magnetron sputter system (6), and thermal desorption analysis of accumulated in the film species is performed in the TDS chamber (7).

2.1 Vacuum system

Both main chambers are pumped out separately using two pumping lines. The deposition chamber is pumped by a turbomolecular pump Pfeiffer HiPace 80 (8), and a high-rate oil free scroll pump ISP-90 (9). The TDS chamber is pumped by two TMP (Pfeiffer HiPace 80 and Leybold i90 (connected in line to increase hydrogen compression ratio) and a membrane pump Pfeiffer MBVP015-4.

The pressures in both chambers is constantly monitored using Pfeiffer PKR251 full range vacuum gauges (10). Deposition chamber is equipped with two capacitance gauges (11) with full ranges of 1 mbar and 1000 mbar. This allows precise monitoring of the pressure during plasma discharge irrespective of the working gas composition in a very wide pressure range with high upper limit.

The ultimate pressure dominated by hydrogen is below 5×10^{-7} Pa in the TDS chamber after a daylong bakeout at 110°C. The ultimate pressure is 2×10^{-5} Pa in the deposition chamber dominated by water vapor. To reduce water vapor pressure, the deposition chamber is equipped with a cryotrap (12). The cryotrap is a cylindrical vessel the total volume of $\sim$ 5.4 liters, and the geometric surface area of $\sim$ 0.2 m^2; the vacuum-facing surface is mirror polished. The cryotrap can be run day and

2020 JINST 15 P01011

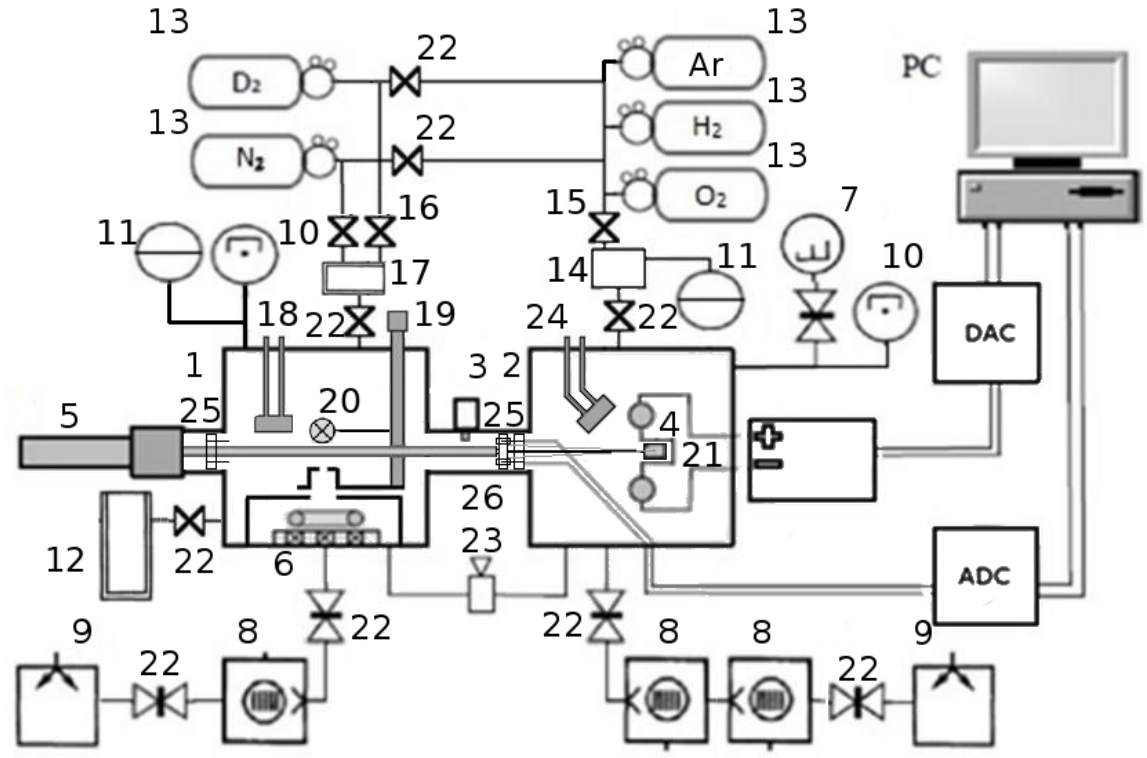

Figure 1. Schematic of the experimental installation MD-2: 1 – deposition chamber, 2 – TDS chamber, 3 – vacuum gate valve, 4 – experimental sample, 5 – linear and rotary feedthrough, 6 – DC planar magnetron, 7 – quadrupole mass spectrometer (QMS), 8 – turbomolecular pump, 9 – roughing pump, 10 – full range (Pirani and cold cathode) vacuum gauge, 11 – capacitance vacuum gauge 12 – cryotrap, 13 – gas bottle, 14 – vacuum volume for QMS calibration, 15 – precision variable gas leak, 16 – gas flow controller, 17 – gas inlet cryotrap, 18 – quartz microbalance deposition monitor (QMB), 19 – rotary feedthrough, 20 – radiative heater, 21 – Π-shaped radiative heater, 22 – vacuum valves, 23 – calibrated leak, 24 – ultra high vacuum quart microbalance deposition monitor, 25 – stationary part of the sample holder, 26 – mobile part of the sample holder.

night continuously for a week or longer with the same target or sample substrate without unfreezing. The cooling media used is liquid nitrogen with the temperature of about 77 K. When active, cryotrap reduces water vapor content by about an order of magnitude. The deposition chamber cannot be baked out if a chemically active element, such as lithium, is used as a sputter target.

The gas inlet system consists of five gas bottles with D_2, N_2, Ar, O_2, H_2, which are attached to the inlet valve (13). As study of deuterium co-deposition was the primary goal of most experiments conducted using MD-2, the deuterium line is separated from other lines. The inlet system is connected to the TDS chamber through a volume (14) for quadrupole mass spectrometer (QMS) calibration and a variable precision leak (15). The inlet system is connected to the deposition chamber using two parallel mass flow controllers RRG-12 (16), one — for deuterium and another — for other gases. The gas is supplied directly to the magnetron system for maximum gas efficiency. The whole system is composed of only metal components and can be baked out. In order to prevent cathode and deposited film poisoning by impurities coming with the gas inflow, a cryotrap (17) is placed in the inlet gas line.

2020 JINST 15 P01011

In addition to gas bottles, a thermochemical water vapor source (TWVS) based on the thermal decomposition reaction $Ca(OH)_2 \leftrightarrow CaO+H_2O$, similar to that described in [25, 26] is connected to the deposition chamber. This allows the study of interaction of deposited films with water vapor under controlled conditions. The TWVS capacity is ~ 40 g of $Ca(OH)_2$, which translates to more than 12 hours of continuous generation of water in the vacuum chamber at 10^{-1} Pa with constant pumping.

2.2 Deposition chamber

The deposition chamber is used for co-deposition of metal films and plasma species using magnetron discharge sputtering. The scheme of the chamber with a magnetron, diaphragms, experimental sample, and quartz microbalance is shown in figure 2.

A cylindrical planar DC magnetron is installed on the bottom flange of the deposition chamber. Permanent Sm-Co magnets are directly cooled by water. The cylindrical magnetron housing is grounded and, together with the walls of the vacuum chamber, serves as the discharge anode. A supplemental discharge between magnetron housing and magnetron sides provides additional electrons for the main magnetron discharge increasing its efficiency. The magnetron is powered by a stabilized DC power supply working either in the constant or in the frequency mode. It can maintain either the constant voltage (V = 0–1000 V with 1 V resolution), or constant current (I = 0–5 A with 0.1 A resolution), or constant power (0–5 kW with 5 W resolution). Normally, power stabilized 100 kHz 80% duty cycle frequency mode is used in the case of chemically active cathodes to prevent discharge instabilities producing droplets.

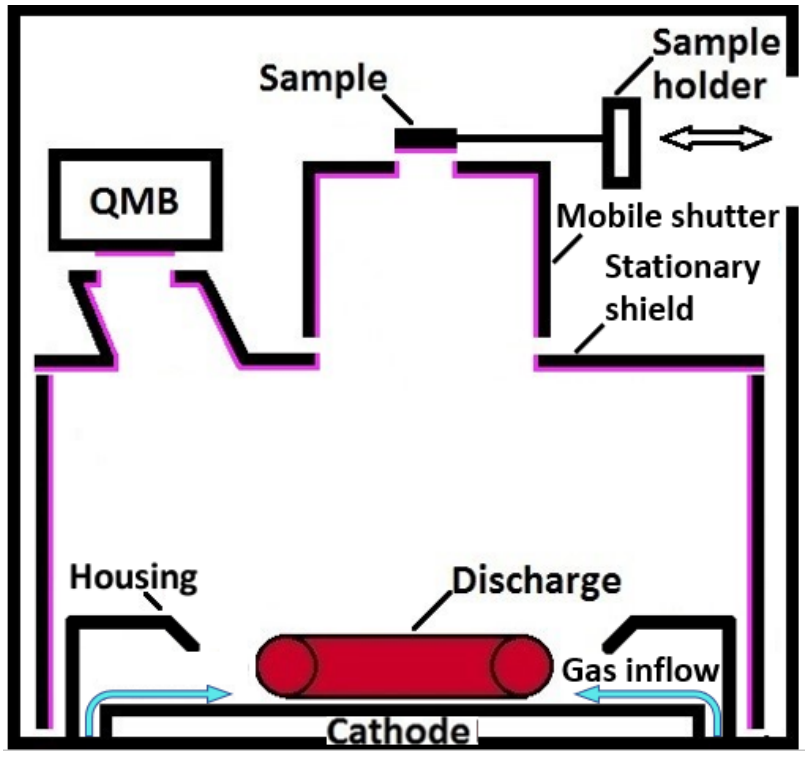

Figure 2. The scheme of the deposition chamber of the MD-2 device. Pink lines indicate areas where material sputtered from the cathode is deposited.

For experiments on hydrogen-solid co-deposition deuterium is used to overcome problems connected with the background signals. Argon is used for sputtering. So, the working gas is a mixture Ar:D ≈ 1:1. For experiments on hydrogen-lithium co-deposition, pure D_2 working gas is used.

The rate of film deposition is monitored using INFICON quartz microbalance (QMB) with 0.1 s time resolution and 10^{-8} g mass resolution (figure 1.18). Thermal shock resistant gold coated quartz crystals are used to allow deposition of very thin chemically active films, such as Li-D co-deposits. To account for differing spatial positions of QMB and experimental sample, additional calibration procedures were carried out as described below.

To prevent metal deposition on unwanted surfaces, the magnetron is surrounded by two shields with orifices in front of the sample and QMB. The shield with the orifice in front of the sample can be shifted to prevent deposition on the sample in the beginning of the discharge when the magnetron target is not clean and the discharge is not stabilized. In the case of liquid Li targets, the sample is shielded to prevent the deposition before the target is melted. The shield in front of the sample can be biased to create a glow discharge between its surface and the sample to clean the sample. Additionally, a radiative heater (figure 1.20), made of a halogen lamp with a molybdenum screen mounted on the rotary feedthrough can be placed behind the experimental sample to heat it during deposition. A supplementary radiative heater made of tungsten wire is positioned on the back side of the experimental sample. It allows the sample to be heated up to ~ 550°C. The sample is also heated by the magnetron discharge, so the heating power can be adjusted to fix the sample temperature at a required level during deposition. For solid magnetron targets, such as W, Mo, Al, the temperature variance during deposition is as low as 2 K. For liquid magnetron targets, such as Li, the variance rises to ~ 15 K due to more unstable heat flux from the magnetron discharge.

The discharge can be monitored visually, through two viewports, and one of them is used also to control the sample surface visually. For example, the white Li-D film becomes dark red after transformation to Li_3N due to reaction with nitrogen.

2.3 TDS chamber

TDS chamber is a high vacuum system separated from the deposition chamber by a gate valve. The sample in the TDS chamber is heated by radiation from a resistive Π-shaped heater (figure 1.21), which is made of 50 μm thick tungsten foil and installed near the center of the chamber. The sample is positioned in the center of the heater. Sample biasing can be used for supplementary heating by electrons. The temperature is measured by a K-type thermocouple spot-welded to the samples. The sample can be heated with the linear increase of the temperature using a feedback system with PID parameters chosen so that there are no oscillations of temperature during heating, which may lead to appearance of false TDS peaks. In order to achieve better stabilization, heating begins 20 seconds after PID feedback is turned on. The typical heat-up rate is 2 K/s.

The walls of the TDS chamber are water cooled to minimize the background signal. The partial gas pressures in the TDS chamber are monitored by QMS. After bakeout, the pressure is dominated by hydrogen. An additional vacuum volume (figure 1.14) for QMS calibration is connected to the TDS chamber by a vacuum valve (figure 1.22). Quadrupole sensitivity is different for different vacuum system configurations, different species, and it can be also different in different experiments. Therefore, QMS requires regular calibration, which is described in detail below.

2020 JINST 15 P01011

Deposition chamber is connected to the TDS chamber by a calibrated leak (figure 1.23) which can be opened to monitor gas composition in the deposition chamber up to the pressures of about 10 Pa. For liquid targets, such as Li, impurities in the working gas can play a significant role [27].

An Inficon Ultra-high vacuum QMB system (figure 1.24) is placed in the TDS chamber, so that the surface of the QMB crystal is in direct line of sight of the experimental sample. It is used to monitor evaporation of the sample during TDS if the sample has a low melting point. The combined TDS-QMB diagnostic is described in detail below.

2.4 Sample transfer system

The deposition chamber and TDS chamber are separated by a gate valve (figure 1.17) that allows to transfer the sample between the two chambers and vent the deposition chamber living the TDS chamber under high vacuum.

The sample transfer system has two stationary parts (figure 1.25), fixed in the chambers, and the mobile part (figure 1.26), which can be moved between the two chambers by the feedthrough (figure 3). The mobile part holds the sample with a thermocouple spot welded to the sample. The stationary parts are used to fix the mobile part in the chambers.

The sample is mounted on a thin (0.5 mm) W frame, which is attached to an insulating rod, which in turn, is mounted on the metal base of the mobile part of the sample transfer system. The mobile part has five electrically isolated metal tubes, which are contacts with respective contact rods of the stationary parts of the transfer system. Four of them are used to connect a K-type thermocouple, which is spot-welded to a backside of the experimental sample. The fifth one is used to bias the sample (up to ±1000 V relative to the ground potential). The mobile part can be attached (screwed) to and detached (unscrewed) from the linear-rotary feedthrough (figure 1.18)

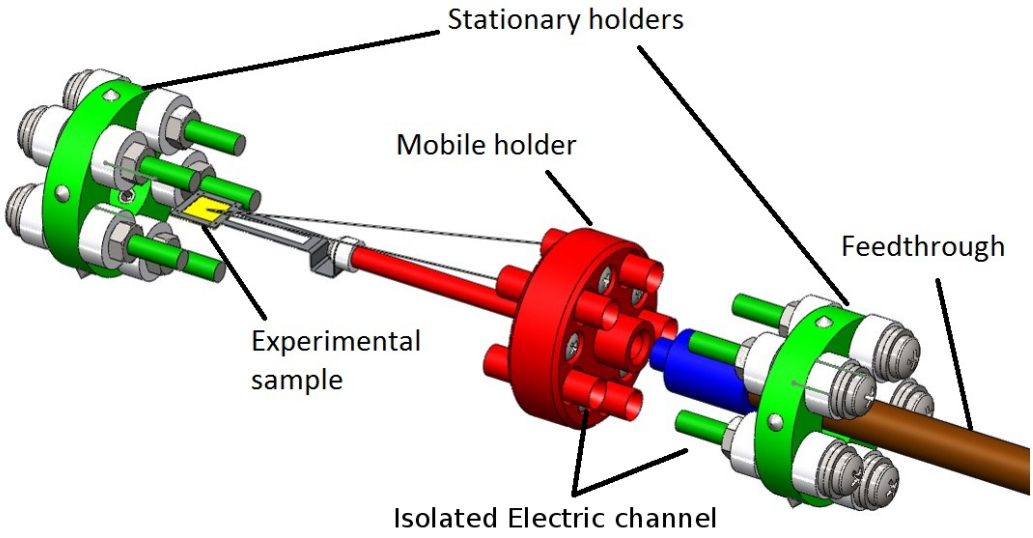

Figure 3. A model of the sample transfer system. Green – stationary parts placed in ports of the chambers, red – mobile part of the sample holder with female screw in the center, blue – male screw tip of the feedthrough rod, brown – main rod of the linear-rotary feedthrough, yellow – experimental sample, white – ceramic insulators. Contacts and insulators of the mobile part are inside the metallic shell and are not shown.

2020 JINST 15 P01011

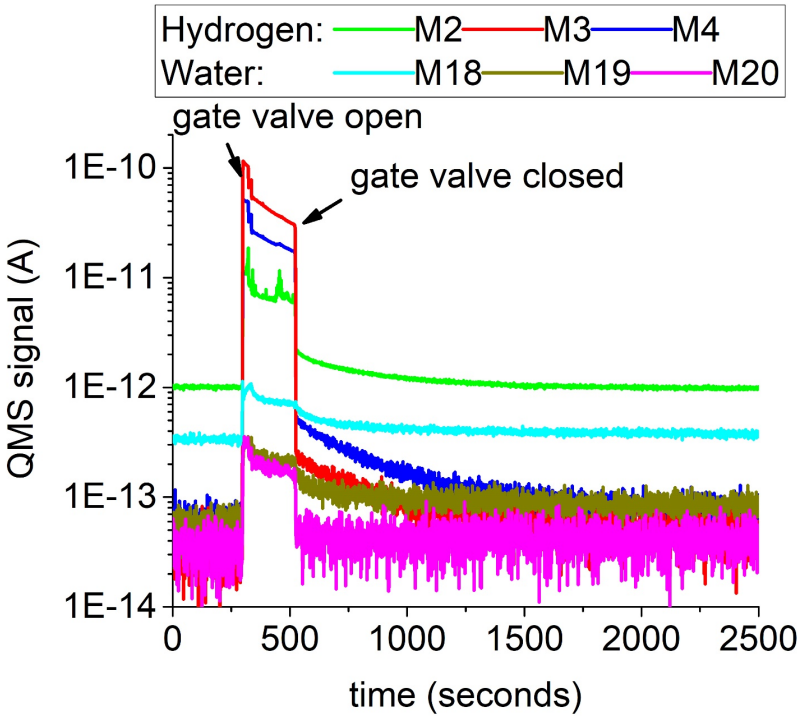

Figure 4. Time evolution of QMS signals of various masses in TDS chamber before, during, and after the experimental sample has been transferred from the deposition chamber into the TDS chamber. Here and below MX stands for the signal of particles with X a.m.u. masses. M2 is taken as protium hydrogen (H_2), M3 as hydrogen deuteride (HD), M4 as deuterium (D_2), M18 as light water (H_2O), M19 as hydrogen-deuterium water (HDO), M20 as heavy water (D_2O).

by its rotation. So, the sample can be transported between the chambers with the gate valve open during transfer and closed both during the deposition and during TDS measurements.

The stationary parts are used to fix the mobile part in the deposition and TDS chambers. They have five electrically isolated metal rods connected to electrical feedthroughs in the chambers, through which thermocouple signals can be read from the sample and bias can be applied. When the rods of the stationary holders are pushed into the tubes of the mobile holder, the mobile holder is fixed and can be screwed to and unscrewed from the linear-rotary feedthrough while remaining in place. During deposition, the mobile part is attached to the feedthrough being connected to the stationary part in the deposition chamber. After deposition, the mobile part is linearly moved into the TDS chamber, attached there to the respective stationary part, and unscrewed from the feedthrough rod. Then the shaft is removed back into the deposition chamber, and the gate valve is closed. This allows to keep good vacuum conditions in the TDS chamber, and to restore it quickly after the sample transfer. Time evolution of QMS signals of various masses before, during and after the experimental sample has been transferred from the deposition chamber into the TDS chamber is shown in figure 4. One can see that the time it takes for the signals to return to their background levels is low, only about 1000 seconds. The stationary part in TDS chamber is positioned between the mobile part of the sample holder and the radiative heater in TDS chamber, and serves as a heat shield, minimizing temperature measurement error.

2020 JINST 15 P01011

The sample itself, which serves as a substrate for the deposited film, is usually a metal plate $10 \times 10 \times 0.2$ mm in dimensions (made e.g. of W). It is fastened to the W frame using 0.05 mm thick W wire through holes in the corners of the sample.

3 Experimental

3.1 Experimental procedure

The quality of the substrate surface can influence the deposited films, especially in the case of deposition of chemically active materials, such as lithium. Therefore, the sample with the spot-welded thermocouple is cleaned in ultrasonic baths in water, gasoline, acetone, and finally in alcohol. Water is used to remove mechanical contaminants, and as a strong solvent for polar molecules. Gasoline is used as a strong solvent to remove nonpolar organic residue. Acetone is used to remove gasoline residue. Finally, alcohol is used to remove water introduced by exposure to acetone, it has the smallest molecule out of all solvents used in the cleaning procedure, also it easily evaporates from the surface. After that, the sample is installed in the deposition chamber. Right before the deposition, the sample is moved into the TDS chamber and baked out at the maximum temperature of 1230°C (limited by the power supply available and the type of thermocouple used) until the QMS signal of 4 a.m.u. decreases to the background level. This also serves the purpose of degassing the TDS chamber itself. For co-deposited films with low melting temperature (such as Li, Al), this ensures evaporation of previously deposited films from the substrate. For co-deposits with high melting temperature (such as W), this procedure ensures degassing and re-crystallization of the deposited film. This means that both for low and high temperature materials, the substrate can be used multiple times with no effect of previous depositions. Using the same substrate multiple times means that there is no need to re-weld thermocouple to the substrate between experiments, which minimizes temperature measurement variance.

Magnetron sputter deposition is performed at the gas pressure of 1 to 5 Pa. After the deposition is finished, the sample is either kept in the constant flow of the working gas for at least 20 minutes or until it cools down to room temperature, whichever is longer. This procedure is used to minimize the effect of the residual gas on the freshly deposited film. Interaction of co-deposited film with gas can be studied if the deposition chamber is filled with the necessary gas. The partial pressures of gases in the deposition chamber are controlled by QMS installed in TDS chamber through a fine leak valve between the deposition and TDS chambers.

After cooling the sample and evacuation of the deposition chamber, the leak valve between the chambers is closed, the sample is moved into the TDS chamber and left there, the feedthrough is moved back into the deposition chamber, the gate valve is closed, and the TDS chamber is pumped out until the QMS signals (typically 4 a.m.u.) return to their background levels. After this, TDS analysis is performed. Simultaneously with TDS measurements, evaporation of non-volatile elements from the analyzed sample is recorded by QMB placed in front of the sample.

To minimize the background, the chambers are baked before experiments. The deposition chamber is baked out while the sample is kept in high vacuum in the TDS chamber. The TDS chamber is baked out before TDS measurements when the sample is in the deposition chamber.

2020 JINST 15 P01011

3.2 QMB calibration

Due to different positions of the sample and QMB with respect to the magnetron, the amounts of sputtered material deposited on QMB and on the sample generally differ. As such, it is required to calibrate the QMS signal with respect to the film mass/thickness on the sample. For this purpose, the amounts of metal deposited on the sample and QMB were measured after test depositions.

To measure small amounts of deposited material, Rutherford backscattering spectroscopy (RBS) was used [28]. The amount of material deposited on the experimental sample was about twice the amount of material deposited on the QMB crystal (1.90 ± 0.08 for Li). It was shown also that the lateral distribution of W film was very uniform over the surface, while Li films became inhomogeneous after contact with air due to chemical reactions with atmospheric gases [28]. The calibration was repeated several times over a period of three years, and the ratio between the amount of material deposited on the experimental sample and the QMB crystal remained constant over that period of time.

3.3 TDS analysis

Because of the small size of experimental samples varied and their low thermal inertia, TDS analysis can be performed with a wide variety of heating rates from ~ 0.1 K/s to about 10 K/s. The limiting factors for the rate of TDS heat-up are: the rate of thermocouple measurements (10 Hz measurement rate is used in MD-2 setup), the rate of QMS measurements, which cannot be increased too much while maintaining high signal to noise ratio (the rate of measurement is about ~ 1 Hz in MD-2 setup), the reaction time of the heating source, and the total time TDS takes. For very long TDS times, over one hour, in-chamber components of TDS setup can be heated and produce high background signal.

3.4 QMS calibration

The main species released in TDS are H_2, HD, and D_2. The contribution of other hydrogen containing gases is usually small. Therefore, the QMS calibration was performed only for D_2 and H_2 gases. To demonstrate the release of all hydrogen containing gases, the signal of QMS measured in Amperes is used.

Thermal desorption measurements are performed in the so-called dynamic regime, where the chamber is pumped out at a relatively high rate, so that the partial pressure in the chamber, which is measured by QMS, is directly proportional to the desorption rate of the respective volatile species. In order to convert QMS signal I [Amperes] into absolute values of volatile species fluxes J [particles/second], calibration of the QMS was performed. The calibration procedure is an upgrade of the procedure described in [24].

Using the variable precision leak (figure 1.22), a gas flow J into TDS chamber is set up, and a respective signal of QMS I is recorded. The value of flow J is selected in a way to produce the signal I typical for that observed during TDS analysis. To measure the absolute value of J, the valve between the calibrated volume (figure 1.3) and the TDS chamber is closed and the pressure rise $p(t)$ in the calibrated volume ($V = 0.0417$ liters) is monitored by an absolute pressure gauge (figure 1.12). If the flux from the bottle to the calibrated volume equals the flux from the bottle to the TDS chamber, the pressure rise dp/dt in the calibrated volume and the gas influx $J = dN/dt$ in

2020 JINST 15 P01011

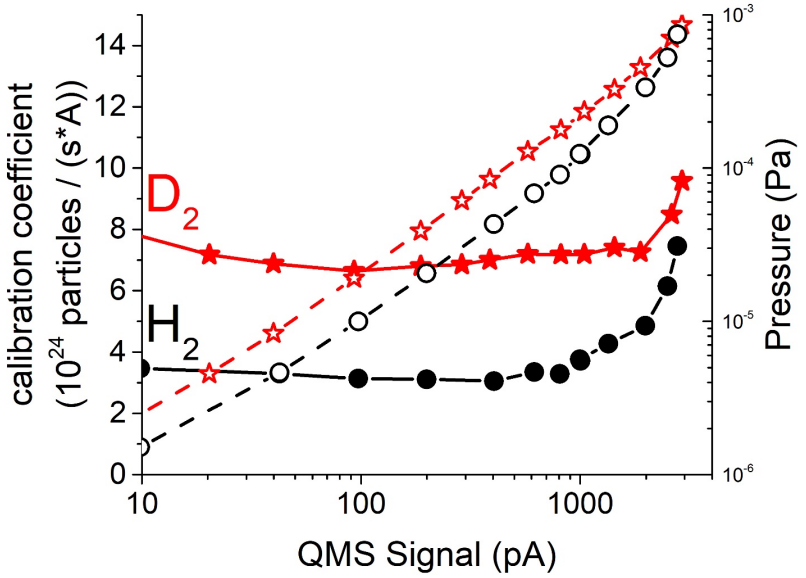

Figure 5. An example of the variation of the calibration coefficients (left axis, solid lines, filled-in points) with the gas pressure (right axis, dashed lines, hollow points) for H_2 and D_2. QMS measurements are performed by Extorr XT100M, pressure measurements are performed by PKR-251 full range gauge.

absolute units are linked as.

$$\frac{dp}{dt} = J\frac{kT}{V}$$

Assuming room temperature of $\sim 295\,\mathrm{K}$, $\frac{dp}{dt}\left[\frac{Pa}{s}\right] = 9.68 \times 10^{-17} J\left[\frac{\text{particles}}{s}\right]$ in our setup. If the gas leak J is proportional to the QMS signal I as $J = c(I)I$, one can calculate the calibration factor $c(I)$ as

$$c(I) = \frac{dp}{dt}\frac{V}{kTI}$$

This factor is then used in the TDS run to calculate the absolute value of the volatile species desorption rate using the QMS signal measured in relative units. The calibration coefficient and the sensitivity of QMS are inversely related. Figure 5 gives an example of the variation of the QMS calibration coefficient with the gas pressure. It should be noted that $c(I)$ changes with pressure, that is the calibration coefficient depends on the conditions of the experiment. Decrease in sensitivity (increase of the calibration coefficient) at high fluxes is a prominent and consistent feature of the calibration curve (figure 5).

This procedure is repeated regularly after each TDS measurement as the QMS sensitivity can vary unpredictably between two experiments as well as it can be different for different fluxes, species, and varies with variations in the arrangement of the vacuum system. This procedure is regularly performed only for H2 and D2. For other masses it is time consuming and can be performed only if it is really necessary.

An example of raw QMS signals during TDS analysis of a Li-D film and absolute values of gas release rates $J = c(I)I$ obtained after calibration is shown in figure 6. One can see that the peak positions and shapes of the curves remain mostly unchanged between raw spectra and calculated gas fluxes. The shape of each individual mass signal spectrum changes slightly, as well as the ratio

2020 JINST 15 P01011

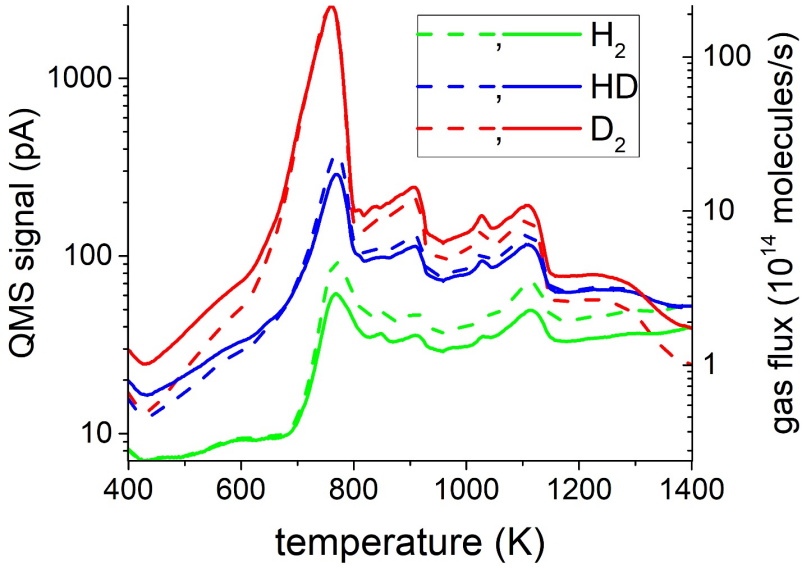

Figure 6. Raw QMS signals (dashed lines, left Y axis) and calculated gas fluxes (right Y axis, solid lines) during a TDS analysis of a Li-D film. Both Y axis are normalized to the full span of the signal.

between signals of different masses: the raw QMS signals suggest lower integral value of high temperature D2 desorption peaks, and lower rate of desorption at low temperature, as well as higher H2 content, than the processed TDS spectra.

3.5 TDS background

The problem of any TDS experiments is the background signal, which can vary during TDS measurements unpredictably, because all materials around the sample are heated. Active water cooling of the chamber walls partially decreases the background signal; however, its minimization remains an important task. In MD-2 device the minimization of the background is achieved by regular bakeout sessions between TDS, where the radiative heater operates at its maximum power. Figure 7 shows the background signals of several masses for two TDS sessions without deposited films — one with the sample holder in the TDS chamber, and another — without the holder in the chamber. One can see that the background signals, which can be connected with walls, are low until the very end of TDS, and the sample holder itself does not add anything significant to the background. That is, TDS measurement in this well-baked system are not influenced by the background.

3.6 In-situ evaporation rate measurement

In order to measure the evaporation rate of analyzed films and to correlate this rate with volatile species desorption, a QMB was installed in the TDS chamber. The use of QMB during TDS runs is complicated by heating of the quartz crystal by radiation from the sample and the sample heater, as the resonance frequency of the crystal is temperature sensitive. Figure 8 shows two dependencies of the QMS signal on the power applied to the sample heater: one curve is for the sample with Li-D film, and another one for the blank sample without the film. One can see that the "mass" on the QMB crystal "decreases" with the power in both cases, even if Li is deposited on the QMB crystal.

2020 JINST 15 P01011

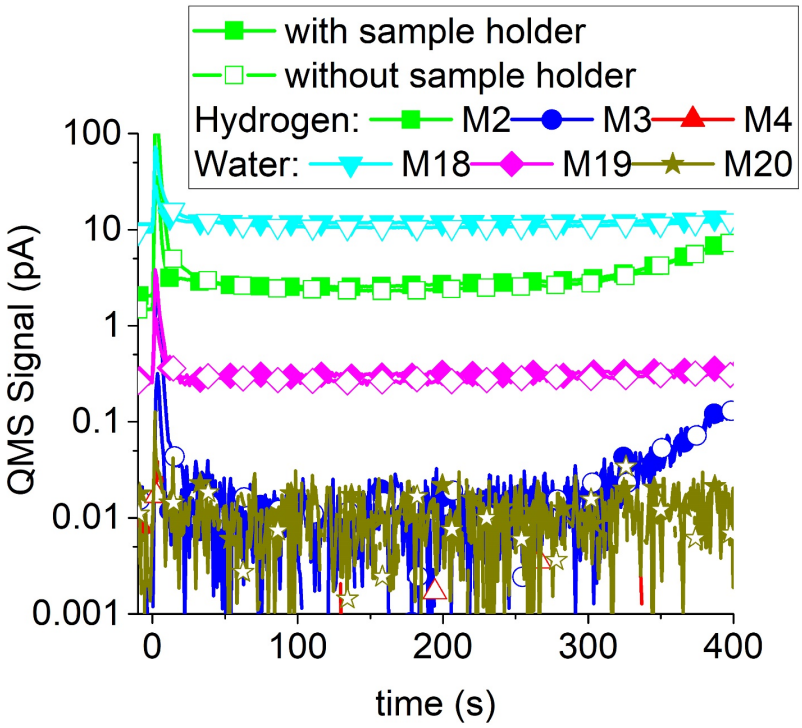

Figure 7. QMS signals of 2, 3, 4, 18, 19, 20 a.m.u. for two identical TDS runs in the well annealed system with and without the sample holder in the TDS chamber (solid and empty dots, respectively). Signal of 4 a.m.u. is below the detection limit. Heating rate for TDS run with the sample holder is 2 K/s. QMS signals are given in amperes, because no calibration for water vapor isotopes was performed.

The difference between the curves with and without the Li film gives the real effect of deposition, which can be recalculated into the rate of Li evaporation from the sample.

One can see from figure 8 that the background is very high, and the Li film deposition gives a very small effect. As the drift depends strongly on how the sample is heated, the blank sample was measured in very similar temperature runs as those used in TDS with co-deposited films. Besides, several measurements (usually three) were made to get good averaging. The true amount of the deposited material and true deposition rate are given by the difference between the two curves.

4 Typical experiments

This section demonstrates three typical experiments: TDS from a film with a low melting temperature, TDS from a film with a high melting temperature, and gas interaction with co-deposited films.

4.1 TDS from co-deposited films with low melting temperatures

Here we demonstrate TDS analysis of $\sim 1\,\mu$m thick Li-D co-deposited film coupled with simultaneous QMB monitoring of evaporation of the film. The example demonstrates how qualitatively new data on hydrogen accumulation can be obtained by combining QMB and TDS measurements.

TDS measurement was performed at the rate of 2 K/s to the maximum temperature of 1350 K, which was sufficient for full evaporation of Li from the substrate. In parallel to QMS, the signal

2020 JINST 15 P01011

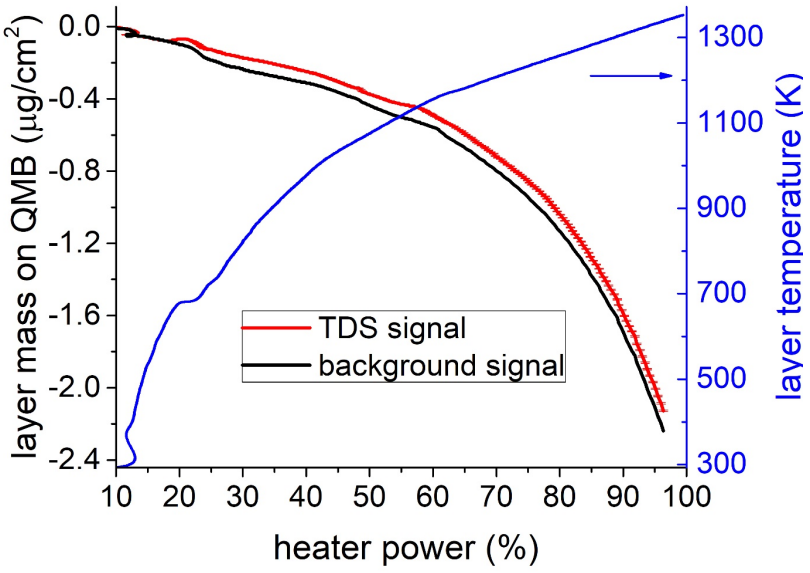

Figure 8. The "deposited mass" as observed by QMB as a function of heater power for the sample with D-Li film (red line) evaporated onto the QMB crystal and the blank sample without any film (black line) where no evaporation onto the QMB crystal took place. Blue line is the sample temperature during heating (right Y axis).

of QMB was recorded to characterize Li-D film evaporation. The results are shown in figure 9. One can see from figure 9 that up to the temperature of ~ 670 K, evaporation dynamics of Li-D film correlates very well with the prediction of the evaporation dynamics of metallic lithium [19]. However, the main deuterium release peak is shifted with respect to the temperature of fastest Li evaporation. This may indicate that Li-D hydride phase exists in the film, which decomposes above the temperature of evaporation of metallic Li. The shoulder from ~ 700 K to ~ 780 K on the Li evaporation curve correlates with the main D_2 desorption peak and can be associated with LiD decomposition [29].

Interpretation of QMB signal at temperatures above 1100 K is less certain, due to a very high background signal drift (figure 8). It might be due to decomposition of Li_3N compound, as signal of 28 a.m.u. was also observed in that temperature range. An alternative explanation for high temperature (up to 1400 K) evaporation of Li may be connected with evaporation of small amounts of Li. Evaporation of sub-monolayer ultra-thin Li films from Mo substrates up to 1400 K was observed directly by direct QMS measurements in [30].

Lithium film had been completely evaporated by the end of TDS. It was mainly deposited on the surfaces of the shield and shutter, and only about 0.3% of the evaporated Li was deposited on the QMB. Though Li is the lightest material to study, it was still possible to measure its evaporation and deposition, indicating the potential of this method for analysis of thin films of low mass and low melting point. Lithium films as thin as ~ 500 nm can be reliably studied. Assuming similar geometry, 50 nm tin films could be analyzed; and the sensitivity can be increased even further with proper adjustments, such as by changing radiative heater to an electron gun heater, and optimization of the setup geometry.

2020 JINST 15 P01011

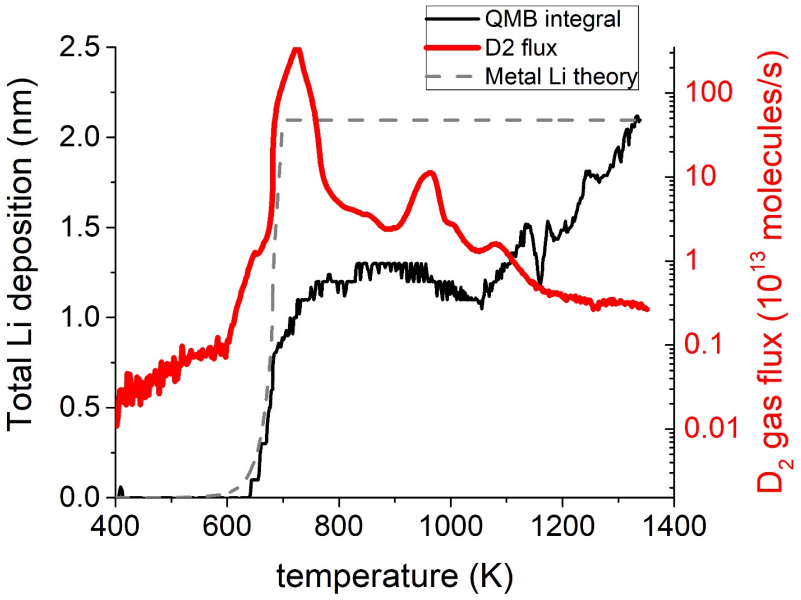

Figure 9. Comparison of the deuterium desorption rate measured by QMS (red, right Y axis) and thickness of the film deposited on the QMB assuming metallic Li density (black, left Y axis) during TDS runs with Li-D film. The grey dashed line – theoretical prediction for Li deposition on QMB assuming evaporation of metallic Li.

4.2 TDS from co-deposited films with high melting temperature

To test the functionality of the installation and quantitative repeatability of the experiments in the case of films with high melting temperature, several W deposition experiments were performed. A tungsten film (approximately 2 μg, as measured by QMB), was deposited using a 99.95% pure W sputter target and D : Ar = 1 : 1 gas mixture.

TDS spectra for 2, 3, 4 a.m.u. measured for a D-W film (co-deposited without additional substrate heating during deposition) are shown in figure 10. For a.m.u. 4, one can see a well pronounced peak at a temperature of about 400 K, and a small shoulder at around 650 K. The signal of the 4 a.m.u. was the highest among all observed masses. Both mass 4, i.e. D_2 and mass 3, i.e. HD were used to calculate the deuterium content. Changes in mass 2 signal were always accompanied by corresponding changes in mass 3 signal, even when HD can be safely assumed to be absent. This can be due to formation of H_3 ions in QMS, or due to insufficient mass resolution of QMS resulting in overlapping of QMS peaks of mass 2 and mass 3. To analyze this effect, a TDS of a sample without D/W film was measured. It was observed that an increase of the QMS signal at the frequency of mass 2 was always accompanied the increase of the signal at the frequency of mass 3, which was 14 times less than that of mass 2. Therefore, $1/14^{\text{th}}$ of the mass 2 signal was subtracted from the mass 3 signal when calculating the release of HD molecules. At the early stage of TDS (first 30 s) hydrogen molecules are likely desorbed from the radiative heater, but not from the analyzed sample (see figure 9), therefore this part of spectra was not taken into account in calculations of the total D amount. The background signal around 4 a.m.u. was below 10^{-14} A (equivalent to $\sim 4{\times}10^{10}$ atoms/s), which was orders of magnitude less than the highest peak of 4 a.m.u., and the integral of background signal for the whole period of TDS was only 2% of the total integral of the 4 a.m.u. signal.

2020 JINST 15 P01011

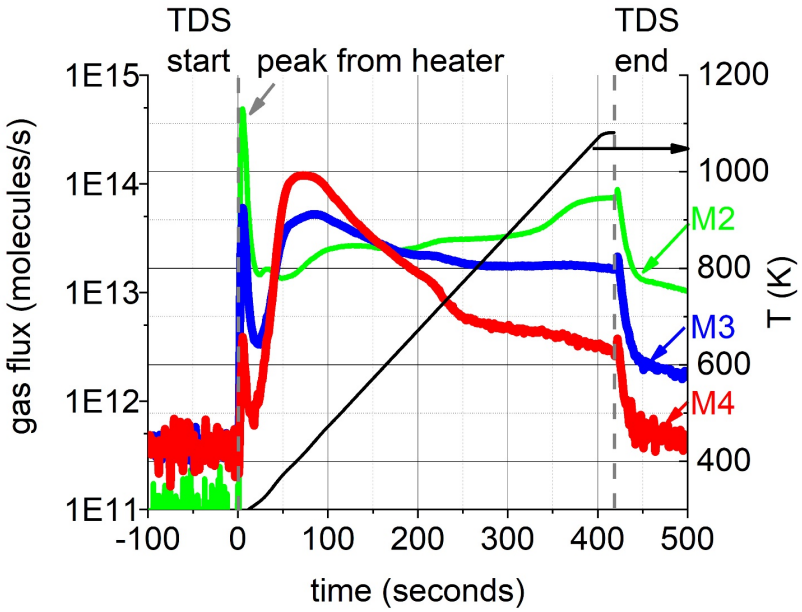

Figure 10. Release rates of 2, 3, 4 a.m.u. in arbitrary units and temperature of the sample vs. time during TDS of a co-deposited D-W film. The heating rate is 2 K/s. Right Y axis shows the temperature of the experimental sample during TDS, the temperature after the end of TDS is not recorded. Vertical dark grey dashed lines represent start and end of TDS process.

The increase in 2 a.m.u. signal near the end of the TDS can be attributed to the background signal. After TDS was finished and the temperature decreased, the signals of all masses rapidly returned to their background levels.

The temperature of the sample vs time is also shown in figure 10. The temperature rise was very close to linear, with minor deviation below 400 K. The linear fit of the experimentally measured $T(t)$ curve resulted in the slope of 2 K/s. The setup required calibration to adjust PID parameters of the feedback system, but, once correct values were obtained, a linear repeatable heat-up was possible.

Because of the good temperature resolution, and the ability to perform depositions and TDS analyses quickly (up to four analyses per day), it was possible to obtain the most detailed (25 K resolution) temperature dependence of deuterium content in W films in the widest temperature range (from near room temperature up to 800 K) ever measured. This gave the opportunity to observe the step-like shape of the curve, which was previously unseen [31, 32]. The new experimental data allowed us to verify a newly developed theoretical model [33] proposed for co-deposition process.

These experiments, as well as experiments on Mo-D and Al-D co-deposition are described in detail in [33, 34].

4.3 Gas interaction with thin films

Interaction of thin films with gases is an important problem in film deposition. In this section an example of investigations of interaction of Li-D co-deposited film with water vapor is given. The film was deposited on QMB in deuterium gas using liquid lithium cathode made as a capillary-porous system [35]. After deposition, water vapor from TWVS was introduced into the deposition

2020 JINST 15 P01011

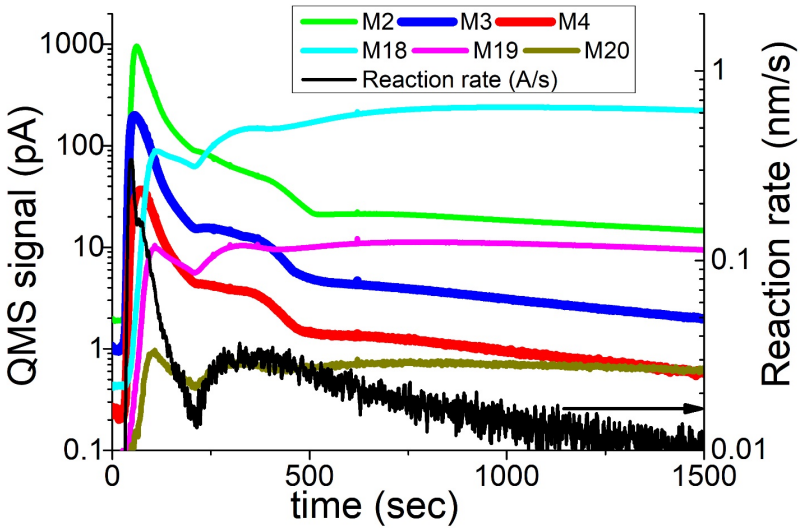

Figure 11. Signals of various masses during interaction of the 100 nm Li-D film deposited on QMB crystal with water vapor. Right Y axis indicates the rate of Li-D film transformation into LiOH, shown as the black line [27].

chamber, and mass of the film on the QMB as well as gas release were measured as a function of time. The experiments were performed at room temperature, with continuous water cooling of the QMB.

From changes in the mass of the film, it is possible to calculate the rate of the reaction with water vapor. Figure 11 shows variation of QMS signals of various masses during interaction of the 100 nm Li-D film with water vapor at room temperature together with the reaction rate. Calibration in this experiment was not performed because the pressure and the QMS signals were measured in different chambers, connected through a fine leak, which was difficult to reproduce from experiment to experiment. Therefore, release rates are given in arbitrary units. The water leak was constant, but H_2O signal rose in time. This means that the initial reaction rate of the Li film with water (black line) was very high, and it decreased gradually for about 250 s. The reaction was accompanied by release of H_2, HD, D_2, HDO, and D_2O. One can observe a very high release rate of deuterium and accumulation of protium in the film, which means isotopic exchange in the film.

After 1500 s, the reaction with water was completed, and the mass of the film increased about 3 times, which can be interpreted as transformation of a mixture of Li (7 a.m.u.), Li-H (8 a.m.u.) and Li-D (9 a.m.u.) into LiOH and LiOD (24 and 25 a.m.u.). Subsequently the deuterium content in the resulting film was measured by TDS, demonstrating significant changes to deuterium desorption compared to normal Li-D co-deposited layer [27].

5 Summary

The high vacuum experimental installation for TDS investigation of thin metal films deposited in gas is described. Deposition can be performed in wide ranges of the deposition rate, gas pressure, and substrate temperature. The TDS analysis is performed in a separate UHV chamber after transportation of the sample from the deposition chamber in vacuo without contact with air. Two

2020 JINST 15 P01011

QMBs were installed both in the deposition and TDS chambers to analyze the film deposition, evaporation, and transformation either during TDS or during reactions with gases

Routine calibration procedures of QMS and QMB signals are described. It is shown that for quantitative measurements, regular calibrations in the whole range of signals are required.

Functionality of the installation and advantages provided by its features were demonstrated in three experiments: 1) trapping of deuterium by the growing chemically active film of Li with subsequent decomposition and evaporation of the film, 2) temperature dependent deuterium trapping in the growing W film resulting in trapping with several binding energies, and 3) chemical interaction of D-Li film with water vapor with isotopic H-D exchange and chemical transformation of the deposited film.

Acknowledgments

The development and testing of QMB-based enhancement of TDS analysis, and upgrade of the water vapor source were supported by Russian Science Foundation grant № 18-72-00213. The development of magnetron sputtering system was supported by grant № 14.Y26.31.0008 given by the Ministry of Education and Science of the Russian Federation.

References

[1] S. Krat et al., *Hydrocarbon film deposition inside cavity samples in remote areas of the JET divertor during the 1999–2001 and 2005–2009 campaigns*, *J. Nucl. Mater.* **463** (2015) 822.

[2] J.P. Coad et al., *Erosion/deposition issues at JET*, *J. Nucl. Mater.* **290–293** (2001) 224.

[3] M. Shimada et al., *In-vessel dust and tritium control strategy in ITER*, *J. Nucl. Mater.* **438** (2013) S996.

[4] J. Likonen et al., *Investigation of deuterium trapping and release in the JET ITER-like wall divertor using TDS and TMAP*, *Nucl. Mater. Energy* **19** (2019) 166.

[5] S. Krat et al., *Beryllium film deposition in cavity samples in remote areas of the JET divertor during the 2011–2012 ITER-like wall campaign*, *Nucl. Mater. Energy* **12** (2017) 548.

[6] A. Widdowson et al., *Overview of fuel inventory in JET with the ITER-like wall*, *Nucl. Fusion* **57** (2017) 086045.

[7] S. Brezinsek et al., *Plasma-wall interaction studies within the EUROfusion consortium: progress on plasma-facing components development and qualification*, *Nucl. Fusion* **57** (2017) 116041.

[8] S. Mirnov, *Tokamak evolution and view to future*, *Nucl. Fusion* **59** (2019) 015001.

[9] F.L. Tabares et al., *Conference Report on the 4rd International Symposium on Lithium Applications*, *Nucl. Fusion* **56** (2016) 127002.

[10] G. Mazzitelli et al., *Conference Report on the 3rd International Symposium on Lithium Application for Fusion Devices*, *Nucl. Fusion* **55** (2015) 27001.

[11] J. Miyazawa et al., *Conceptual design of a liquid metal limiter/divertor system for the FFHR-d1*, *Fusion Eng. Des.* **125** (2017) 227.

[12] J.P.S. Loureiro et al., *Behavior of liquid Li-Sn alloy as plasma facing material on ISTTOK*, *Fusion Eng. Des.* **117** (2017) 208.

2020 JINST 15 P01011

[13] I. Zammuto et al., *Implementation of ferritic steel as in vessel wall: Lessons learnt and follow up*, *Fusion Eng. Des.* **124** (2017) 297.

[14] J. Roth, K. Sugiyama, V. Alimov, T. Höschen, M. Baldwin and R. Doerner, *EUROFER as wall material: Reduced sputtering yields due to W surface enrichment*, *J. Nucl. Mater.* **454** (2014) 1.

[15] V.Y. Sergeev et al., *Conceptual design of divertor and first wall for DEMO-FNS*, *Nucl. Fusion* **55** (2015) 123013.

[16] S.A. Krat, Y.M. Gasparyan, A.S. Popkov and A.A. Pisarev, *Deuterium release from lithium-deuterium films, deposited in the magnetron discharge*, *Vacuum* **105** (2014) 111.

[17] A.M. Capece, J.P. Roszell, C.H. Skinner and B.E. Koel, *Effects of temperature and surface contamination on D retention in ultrathin Li films on TZM*, *J. Nucl. Mater.* **463** (2015) 1177.

[18] A.B. Martín-Rojo, E. Oyarzabal and F.L. Tabarés, *Laboratory studies of H retention and LiH formation in liquid lithium*, *Fusion Eng. Des.* **89** (2014) 2915.

[19] I.E. Lyublinski, A.V. Vertkov and V.A. Evtikhin, *Application of lithium in systems of fusion reactors. 1. Physical and chemical properties of lithium*, *Plasma Devices Oper.* **17** (2009) 42.

[20] R.A. Lidin, V.A. Molochko and L.L. Andreeva, *Reactions of Inorganic Compounds*, 2nd edition, R.A. Lidin ed., DROFA, Moscow (2007).

[21] A.S. Popkov, S.A. Krat, Y.M. Gasparyan, Y.A. Vasina and A.A. Pisarev, *On the interaction of Li-D films with nitrogen and oxygen at room temperature*, *J. Surf. Investig.* **10** (2016) 860.

[22] S.A. Ryabtsev, Y.M. Gasparyan, Z.R. Harutyunyan, I.M. Timofeev, O.V. Ogorodnikova and A.A. Pisarev, *Deuterium thermal desorption and re-emission from RAFM steels*, *Phys. Scripta* **T170** (2017) 014016.

[23] A.V. Tumarkin, A.V. Kaziev, D.V. Kolodko, A.A. Pisarev, M.M. Kharkov and G.V. Khodachenko, *Deposition of copper coatings in a magnetron with liquid target*, *Phys. Atom. Nuclei* **78** (2015) 1674.

[24] A.A. Rusinov, Y.M. Gasparyan, S.F. Perelygin, A.A. Pisarev, S.O. Stepanov and N.N. Trifonov, *A setup for thermodesorption measurements*, *Instrum. Exp. Tech.* **52** (2009) 871.

[25] G.S. Voronov et al., *Testing of the method for water microleakage detection from OH hydroxyl spectral lines at the L-2M stellarator*, *Plasma Phys. Rept.* **39** (2013) 277.

[26] V. Kurnaev et al., *Spectroscopic localization of water leaks in iter*, *Fusion Eng. Des.* **88** (2013) 1414.

[27] S.A. Krat, Y.M. Gasparyan, A.S. Popkov and A.A. Pisarev, *Time-resolved studies of deuterium release from lithium films exposed to water vapor*, *Fusion Eng. Des.* **124** (2017) 333.

[28] S. Krat, M. Mayer, Y. Vasina, A. Prishvitsyn, Y. Gasparyan and A. Pisarev, *Elastic backscattering as a method for the measurement of the integral lithium content in thin films on fusion-relevant substrates*, *Nucl. Instrum. Meth.* **B 455** (2019) 124.

[29] J.P. Tonks, M.O. King, E.C. Galloway and J.F. Watts, *Corrosion studies of LiH thin films*, *J. Nucl. Mater.* **484** (2017) 228.

[30] O. Fasoranti and B.E. Koel, *Thermal stability of Li films on polycrystalline molybdenum substrates*, *J. Nucl. Mater.* **509** (2018) 532.

[31] V.K. Alimov, J. Roth, W.M. Shu, D.A. Komarov, K. Isobe and T. Yamanishi, *Deuterium trapping in tungsten deposition layers formed by deuterium plasma sputtering*, *J. Nucl. Mater.* **399** (2010) 225.

[32] G. De Temmerman and R.P. Doerner, *Deuterium retention and release in tungsten co-deposited layers*, *J. Nucl. Mater.* **389** (2009) 479.

2020 JINST 15 P01011

[33] S. Krat, Y. Gasparyan, Y. Vasina, A. Davletiyarova and A. Pisarev, *Tungsten-deuterium co-deposition: Experiment and analytical description*, *Vacuum* **149** (2018) 23.

[34] Y. Gasparyan, S. Krat, A. Davletiyarova, Y. Vasina and A. Pisarev, *Temperature dependence of hydrogen co-deposition with metals*, *Fusion Eng. Des.* **146** (2019) 1043.

[35] V. Evtikhin, I. Lyublinski, A. Vertkov, S. Mirnov and V. Lazarev, *Technological aspects of lithium capillary-pore systems application in tokamak device*, *Fusion Eng. Des.* **56–57** (2001) 363.

2020 JINST 15 P01011